Simple and Green Preparation of ZnO Blended with Highly Magnetic Silica Sand from Parangtritis Beach as Catalyst for Oxidative Desulfurization of Dibenzothiophene

Wega Trisunaryanti[1*], Safa Annissa Novianti[1], Dyah Ayu Fatmawati[1], Triyono Triyono[1], Maria Ulfa[2], and Didik Prasetyoko[3]

[1]*Department of Chemistry, Faculty of Mathematics and Natural Sciences, Universitas Gadjah Mada, Sekip Utara, Yogyakarta 55281, Indonesia*

[2]*Department of Chemistry Education, Faculty of Teacher Training and Education, Sebelas Maret University, Jl. Ir. Sutami 36A Surakarta 57126 Indonesia*

[3]*Department of Chemistry, Faculty of Science and Data Analytics, Sepuluh Nopember Institute of Technology, Keputih, Sukolilo, Surabaya 60111, Indonesia*

** **Corresponding author:***

email: wegats@ugm.ac.id

Received: October 23, 2021
Accepted: December 16, 2021

DOI: 10.22146/ijc.69938

Abstract: *Simple and green preparation of ZnO blended with Parangtritis beach sand (BS) catalysts for oxidative desulfurization of dibenzothiophene (ODS-DBT) has been conducted. The ZnO-BS catalysts were prepared by blending ZnO with beach sand under a weight ratio of 1:1, 1:2, and 1:4, and then heated by microwave (MW) at 540 watts for 30 min, resulting in BS-MW, ZnO-MW, ZnO-BS-1-MW, ZnO-BS-2-MW, and ZnO-BS-4-MW, respectively. As a comparison, the ZnO-BS-1 was also heated by oven at 100 °C for 30 min produced ZnO-BS-1-OV. Each product was characterized by XRF, XRD, FTIR, acidity test by NH_3 vapor adsorption, SAA, SEM-EDX, TEM, and magneticity test by an external magnetic field. Furthermore, each material was applied for ODS-DBT, and its product was analyzed by UV-Vis spectrophotometer and FTIR. The results showed that ZnO-BS-1-OV had the highest acidity of 2.3486 mmol/g and produced the highest DBT removal efficiency through the ODS reaction of 81.59%. The use of catalysts in ODS-DBT does not affect the main structure of the treated fuel. Therefore, the combination of ZnO with BS can provide good performance in ODS activity and facilitate the separation of catalysts after the reaction due to its magnetic iron oxide content.*

Keywords: *dibenzothiophene; magnetic; oxidative desulfurization; Parangtritis beach sand; ZnO*

■ INTRODUCTION

One of the world's most critical issues is the depletion of petroleum-based resources due to extended industrialization and motorization. It has been stated that the transport sector uses 40% of the number one energy consumed withinside the world [1]. The decline in oil reserves worldwide increases the dependence on heavy oils containing a heteroatom. Therefore, the trend towards converting heavy oil to light products as much as possible to compensate for this shortage has become a priority in energy research centers. Thus, the percentage of total sulfur content in these refined products increased [2].

The presence of sulfur compounds in transport fuels is undesirable from an environmental side. These sulfur compounds present in fuels such as gasoline and diesel result in harmful effects such as corrosion of engine parts, wear, deposits formation, and air pollution. These environmental risks have led the environmental protection agency (EPA) to set the maximum sulfur content in gasoline to less than 30 ppm. At the same time, this ratio was determined in diesel fuel below 15 ppm [3], and accordingly, refineries have adopted several techniques to meet these legislations. Complete knowledge regarding their structure and chemical nature is desirable to remove these sulfur compounds

from engine fuels by an appropriate refining process. Petroleum oil refineries convert many heavy oils into high-value products that can meet societal needs such as liquid petroleum gas, gasoline, diesel, and jet fuel through physical processes such as distillation or chemical processes such as catalytic reforming [4].

In industry, sulfur compounds are eliminated through the hydrodesulfurization (HDS) method. However, it has a few inherent issues in treating sulfur-containing aromatic hydrocarbon compounds, including dibenzothiophene (DBT) and its derivatives. It also requires harsh conditions, including high temperatures and pressures of hydrogen gas, to provide light oil with low levels of sulfur compounds. Because of this, it's been an urgent challenge to discover new methods for the desulfurization of fuel oils. Catalytic oxidative desulfurization (ODS) combined with extraction of oxygenated sulfur using a polar solvent is considered due to favorable operating conditions. Generally, ODS processes are achieved through the oxidation of sulfur compounds to sulfoxides and sulfones, followed by a separation process using appropriate extractants or adsorbents. ODS is capable of removing the widest possible sulfur compounds due to the nature of the reaction and the ability to operate under mild operating conditions with the presence of green oxidants [5]. According to the literature, various ODS systems have been developed, such as a series of heteropolyacid catalysts, ionic liquids systems, acetic acid catalyst [6-7], porous glass supported with titanium silicate particles [8], and ultrasound-assisted ODS processes [9].

Several solid catalysts had been examined for ODS reaction, including heteropoly acid, either alone or supported [10], and metal oxides, i.e., oxides of (Mo, Mn, Sn, Fe, Co, Zn) metals [11-13]. However, most of it either involved complicated and multistep synthesis techniques or was unrecyclable. The latest literature survey shows that ZnO as a catalyst has obtained significant interest due to its inexpensive, non-toxic, and environmental benefits, i.e., minimal execution time, low corrosion, waste minimization, recycling of the catalyst, clean delivery, and disposal of the catalyst [14]. Parangtritis beach sand is rich in iron, silica, and alumina oxide. It is selected as the support material for ZnO catalyst since it is a reasonably-priced, environmentally friendly, natural active catalyst, and an example of higher use of natural resources [15].

Iron oxide can activate a considered clean oxidant such as H_2O_2, producing active superoxide/peroxide species [16], while the ZnO was reported for adsorptive desulfurization [17]. ZnO is also found to be able to remove the sulfur content without changing the main hydrocarbon structure where non-sulfur-containing crude fuel oil mass remains unchanged. Thus, the combination of the adsorptive capability of zinc oxide and oxidant activated by rich iron oxide sand will enhance the possibility of efficient removal of a refractory sulfur compound through the ODS technique. In addition, iron-zinc oxide material was reported in the literature to have both hydrophobic-hydrophilic characteristics [16]. It has a great potential to act like a phase-transfer catalyst, which is further important for the reaction that consists of immiscible H_2O_2 containing H_2O and hydrocarbon solution.

Therefore, in this research, the ZnO-beach sand catalysts were prepared by the physical grinding (blending) method, which is a simple and easy method that can also provide magneticity properties that allow catalyst recovery at the end of the ODS-DBT reaction so that it can be easily separated from the product by an external magnetic bar. The comparison of catalysts' characteristics and activities heated by microwave at various weight ratios and heated by oven were also studied.

■ EXPERIMENTAL SECTION

Materials

The materials used in this research were sand obtained from Parangtritis Beach, Bantul Regency, Special Region of Yogyakarta with purity can be seen from the XRF data, zinc oxide (ZnO 99% purity, Merck), dibenzothiophene ($C_{12}H_8S$ 98% purity, Merck), *n*-hexane (C_6H_{14} 96% purity), 30% (w/w) hydrogen peroxide (H_2O_2 29–32% purity, Merck), acetonitrile (C_2H_3N 99.9% purity, Merck), distilled water (H_2O, technical grade), ice and filter paper (Whatman Filter Paper, Grade 42).

Instrumentation

Beach Sand (BS) was analyzed by an X-Ray Fluorescence spectrometer (XRF, RIGAKU-NEX QC+QuanTEZ). All catalysts (BS, BS-MW, ZnO, ZnO-MW, ZnO-BS-1-OV, ZnO-BS-1-MW, ZnO-BS-2-MW, and ZnO-BS-4-MW) were analyzed by X-Ray Diffractometer (XRD, Philips X'Pert MPD), Fourier-Transform Infrared Spectrometer (FTIR, Shimadzu IRPrestige-21), acidity test, and external magnetic field. ZnO-BS-1-OV and ZnO-BS-1-MW were analyzed by Surface Area Analyzer (SAA, JW-BK112) and Scanning Electron Microscope-Energy Dispersive X-Ray (SEM-EDX, Hitachi SU 3500). ZnO-BS-1-OV as the best catalyst was analyzed by Transmission Electron Microscopy (Jeol JEM-1400 TEM).

Procedure

Catalyst synthesis

The sand collected from Parangtritis Beach, Yogyakarta, Indonesia, was washed from any excess chloride (Cl^-) using distilled water. It was then dried at 100 °C overnight to remove any excess water on the surface of the beach sand (BS). ZnO was blended with BS in different weight ratios of 1:1, 1:2, and 1:4 and then heated by microwave. The preparation of blended ZnO-BS was carried out as follows: 1 g of ZnO was added by 1, 2, and 4 g of BS and blended homogeneously. Distilled water (1 mL) was added to the mixture to form a paste and then microwaved at 540 watts for 30 min, producing ZnO-BS-1-MW, ZnO-BS-2-MW, and ZnO-BS-4-MW, respectively. BS and ZnO were also heated by a microwave that produced BS-MW and ZnO-MW. ZnO-BS-1 catalyst was also prepared without microwave irradiation (oven), producing ZnO-BS-1-OV.

Catalytic activity test

The model compound dibenzothiophene (DBT) was dissolved into *n*-hexane to make a stock solution of model fuel with a sulfur content of 500 ppm (DBT content = 2874.5 ppm). The oxidative desulfurization (ODS) experiment was performed in a three-necked 500 mL round-bottomed flask equipped with a condenser fitted with a magnetic stirrer and immersed in an oil bath controlled by a thermometer. The mixture of 25 mL DBT and 0.15 g catalyst was then introduced and heated under vigorous stirring. Once the temperature reached 60 °C, 0.12 mL of 30% aqueous solution of H_2O_2 as oxidant was introduced for 20 min under stirring. The oxidized DBT solution was then transferred to a separating funnel followed by the addition of acetonitrile and extracted three times with the volume ratio of the total solvent to oxidized ODS solution of 1:1. The hydrocarbon layer of the oxidized DBT solution was then subjected to quantitative and qualitative analysis.

The hydrocarbon layer of the oxidized DBT solution after extraction was subjected to two different analysis methods. Ultraviolet-visible (UV-Vis) spectrophotometer was used to determine the efficiency of DBT removal. The removal percentage of DBT is calculated based on the following equation:

$$(\%) = \frac{C_0 - C_t}{C_0} \times 100\%$$

where C_0 is the DBT initial concentration in the stock solution and C_t is the DBT concentration of the oxidized DBT solution in the hydrocarbon layer after reaction time (t). In addition to UV-Vis spectrophotometry, the hydrocarbon layer after the reaction was also subjected to FTIR to determine the stability of DBT in *n*-hexane qualitatively.

■ RESULTS AND DISCUSSION

Catalysts Characterization

The crystallographic interpretations were performed by X-ray diffractometer (XRD) using Cu Kα wavelength and scanning in 2θ range from 10° to 80° with a rate of 4°/min. Each diffractogram of the material is shown in Fig. 1.

BS and BS-MW spectra exhibit peaks at 2θ of 8.46, 18.53, 18.73, 22.39, 24.09, 24.62, 28.37, 29.37, 29.57, 29.80, 30.45, 31.04, 33.21, 34.27, 34.74, 35.04, 35.35, 36.37, 36.59, 37.21, 37.42, 37.77, 40.87, 43.38, 43.61, 47.70, 49.38, 53.96, 54.17, 56.21, 57.63, 62.07, 63.88, 64.25, 66.31, 69.42, 71.34, 72.08, 72.33, 74.85, 75.13, 75.28, 79.78, and 80 degrees confirmed that the sand is mainly containing Magnetite (Fe_3O_4), Hematite (Fe_2O_3), Schwertmannite ($Fe_8O_8(OH)_6{\cdot}nH_2O$), and Lepidocrocite (γ-FeO(OH)) with the three strongest peaks showed as

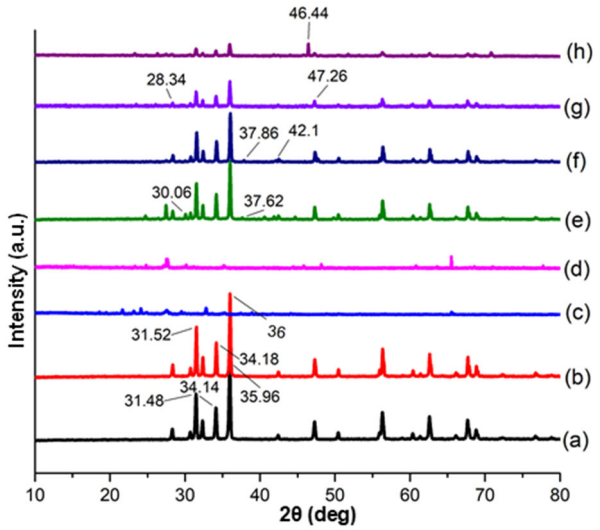

Fig 1. X-ray Diffractogram of (a) ZnO, (b) ZnO-MW, (c) BS, (d) BS-MW, (e) ZnO-BS-1-OV, (f) ZnO-BS-1-MW, (g) ZnO-BS-2-MW, and (h) ZnO-BS-4-MW

Schwertmannite, Lepidocrocite, and Hematite. The observed peak positions match the Crystallography Open Database (COD) File No. 00-101-1032, 00-101-1267, 00-901-5185, and 00-901-5156. ZnO-BS-4-MW material displays a clear appearance of the phase of cubic-$ZnFe_2O_4$ with peaks corresponding to hkl: (111), (220), (311), (222), (400), (331), (422), (531), (442), (620), (533), (642), and (731) with d values of 0.500, 0.300, 0.254, 0.244, 0.193, 0.172, 0.143, 0.141, 0.132, 0.128, 0.012, and 0.109 nm, respectively. The crystal structure of cubic-$ZnFe_2O_4$ is in accordance with the standard COD file no. 00-151-3087 (lattice constant: a = 0.843 nm) [18]. In ZnO-BS-2-MW, the diffractogram shows that the extra peaks also evolved corresponding to (220) (d = 0.302 nm), (331) (d = 0.196 nm), and (642) (d = 0.863 nm) of cubic-$ZnFe_2O_4$. The diffraction spectrums of the blended ZnO-BS-MW samples could not be assigned clearly as Fe_2O_3 due to the amount of Fe^{3+} of BS used in the mixture is very small. In ZnO-BS-1-MW, the diffractogram reveals that the particles form hexagonal-ZnO, also extra planes corresponding to (222) (d = 0.237 nm) and (400) (d = 0.214 nm) are also evolved. In addition to the hexagonal, the phase in ZnO-BS-1-OV develops as extra planes corresponding to (220) (d = 0.297 nm) and (222) (d = 0.238 nm) from cubic-$ZnFe_2O_4$. In the ZnO-MW, the most intense peaks were located at 2θ of 31.49, 34.14, and 35.98 degrees which corresponded to the Miller index of (100), (002), and (101), whereas ZnO lies at 2θ of 31.44, 35.93, and 56.30 degrees which correspond to the Miller index of (100), (101), and (2-10), respectively. The most intense and sharp peaks in Fig. 1 show that ZnO and ZnO-MW have high crystalline and purity. These peaks were identified by comparison with the ICDD powder diffraction file for ZnO (No. 10800075) which confirmed that the particles conform to the hexagonal structure of ZnO (wurtzite type: a = 0.32 nm, c = 0.52 nm). These hkl planes include (100), (002), (101), (102), (2-10), (103), (200), (2-12), (201), (202) with d values of 0.276, 0.262, 0.249, 0.192, 0.163, 0.148, 0.141, 0.138, 0.136, and 0.124 nm, respectively.

From Table 1, it can be seen that microwave treatment can reduce the crystallinity of the material as happened in BS→BS-MW, ZnO→ZnO-MW, and ZnO-BS-1-OV→ZnO-BS-1-MW. The decrease in crystallinity indicates the occurrence of crystalline amorphization. The level of crystallinity is also affected by the ratio of the weight of ZnO to BS. The greater content of ZnO in the mixture will increase the crystallinity. This is because ZnO dominates the crystals more than BS, which is an amorphous material.

The crystallite size of each material from XRD data was calculated using the Debye-Scherrer equation as follows:

$$D = \frac{K\lambda}{\beta \cos\theta}$$

where D is crystallite size in nm, K is Scherer constant (0.89), λ is the X-ray wavelength for Cu-Kα in nm (λ = 1.54059 Å), β is the Full Width at Half Maximum (FWHM) in radian, and θ is the Bragg angle in radian.

From Table 1, it can be concluded that microwave heating can increase the crystallite size of the material, as happened in BS→BS-MW and ZnO→ZnO-MW. The increase in crystallite size is possible for sintering due to the large energy generated by the microwave. Although ZnO-BS-1-OV→ZnO-BS-1-MW has decreased, this value is considered consistent because its difference is very small (0.34 nm). When ZnO is blended with BS, the sintering can be prevented because the position of ZnO and BS could be distributed evenly. The lower the ZnO

Table 1. Crystallinity properties and acidity of materials

Material	Crystallinity (%)	Crystallite size (nm)	Acidity (mmol/g)
ZnO	96.87	38.70	2.1137
ZnO-MW	93.89	51.60	1.9963
BS	76.20	56.54	2.2312
BS-MW	66.00	127.89	2.1785
ZnO-BS-1-OV	90.36	51.22	2.3486
ZnO-BS-1-MW	88.34	50.88	1.7614
ZnO-BS-2-MW	74.91	49.96	1.7826
ZnO-BS-4-MW	74.81	85.21	1.9251

content in the mixture, the more evenly distributed on the BS surface, so the crystallite size will be smaller. On the other hand, the greater the ZnO content in the mixture, the greater the chance of forming aggregates on the BS surface so that the crystallite size increases. This argument does not occur in the case of ZnO-BS-4-MW because ZnO may not be homogeneously distributed on the BS surface.

All materials that have been prepared are tested for acidity using the gravimetric method by ammonia adsorption. The acidity value is expressed as the number of mmol of ammonia absorbed in grams of catalyst. Table 1 summarizes the order of the acidity of the material. Heating the material by microwave can reduce acidity, as happened in BS→BS-MW, ZnO→ZnO-MW, and ZnO-BS-1-OV→ZnO-BS-1-MW. This might happen due to ZnO's dielectric properties by microwave heating, as stated by Omran et al. [18]. The dielectric values of ZnO at room temperature were relatively low. The influence of temperature on the real (ε′) and imaginary (ε″) permittivities indicated that temperature has a more significant effect on the imaginary permittivity than on the real permittivity, and the effect of temperature is more significant at higher temperatures. Due to the low dielectric values of the sample, ZnO is a poor microwave absorber which makes the acidity of the samples decrease when irradiated by microwave. In addition, acidity is also influenced by the weight ratio of ZnO to BS. The acidity will increase following the amount of BS content in the mixture. This is because the largest content in BS is Fe, where this metal contributes a lot of Lewis acid sites from its empty p orbitals. The large amount of ZnO in the mixture allows the formation of aggregates that cover the acid sites of the pores of the material, thereby reducing the acidity.

XRF is used to determine the elemental composition contained in Parangtritis beach sand (BS). The analysis results are shown in Table 2, which implies that the largest elemental contents include Fe, Si, and Al. This proves that BS contains a lot of Fe, which can be applied as potential catalyst support for oxidative desulfurization (ODS) [19-20].

EDX was conducted to compare the elemental content in ZnO-BS-1-OV and ZnO-BS-1-MW. From Table 3, it can be seen that the content of Fe and Zn elements did not change, which indicates that the microwave treatment did not affect the content of both elements in the material. The second reason is possibly the EDX measurement area was not taken correctly, so it is not representative.

Table 2. XRF analysis result of beach sand (BS)

Element	Composition (wt.%)
Al	3.17
Si	11.85
Fe	27.79
Co	0.11
Ni	<0.1
Zn	0.04

Table 3. EDX analysis results of ZnO-BS-1-OV and ZnO-BS-1-MW

Material	Elemental content (wt.%)				
	O	Al	Si	Fe	Zn
ZnO-BS-1-OV	26.5	4	2.4	0.9	66.2
ZnO-BS-1-MW	24.5	4.3	4.1	0.9	66.2

FTIR analysis was applied to determine the functional groups present in the material. According to the literature, magnetite displays two strong absorption bands at 570 and 390 cm^{-1} leading to the Fe–O stretching mode of the tetrahedral and octahedral sites, respectively [21]. Whereas maghemite, a defective form of magnetite, has absorption bands at 630, 590, and 430 cm^{-1}. Geothite contains stretching vibrations of –OH at 3125 (υ–OH), 890 (δ–OH), and 800 (γ–OH) cm^{-1} [22], where the last two bands are important diagnostic bands of goethite as well as stretching Fe-O with weak intensity around 400 and 630 cm^{-1} [23]. Due to their differences, FTIR is considered as one of the suitable tools for confirming the purity of the pure or mixed iron oxide-based material.

By analyzing the spectrum in Fig. 2, it can be stated that the BS consists of a mixture of magnetite and maghemite, based on the fact that the band located at 540.07 cm^{-1} is not symmetric; some weak bands of maghemite may also be present. There is a shift to 524.64 cm^{-1} in BS when heated by microwave. The spectra of BS and BS-MW show water molecule stretching and bending vibrations of protons in hydroxyl at 3448.72 cm^{-1} [24] and –OH vibration bands at 786.96 and 794.67 cm^{-1}. This can be due to the formation of metal hydroxides as an intermediate compound before the formation of ZnO. The C=O stretching between 1543.05 and 1635.64 cm^{-1} and the C–O asymmetric stretching between 1381.03 and 1388.75 cm^{-1} are also present [25]. The bands observed at 2337.72 and 2368.59 cm^{-1} are attributed to the C=O stretching mode, possibly due to the absorption of CO_2 from the air by the metallic cation [26-27]. The absorption band observed at 424.34–447.49 cm^{-1} is associated with the vibrational mode characteristic of Zn–O bonding [28].

In this research, an attempt was made to measure the infrared spectra of ammonia adsorbed on BS, BS-MW, ZnO, ZnO-MW, ZnO-BS-1-OV, ZnO-BS-1-MW, ZnO-BS-2-MW, and ZnO- BS-4-MW surfaces and to investigate the adsorbed state of ammonia on the surfaces of the catalysts. The bands observed at 3448.72–3456.44 cm^{-1} involve both the –OH stretching vibration of surface hydroxyls bonded to NH_3 molecules through hydrogen bonding and the –NH stretching vibration of the adsorbed NH_3 molecules. The absorption band at

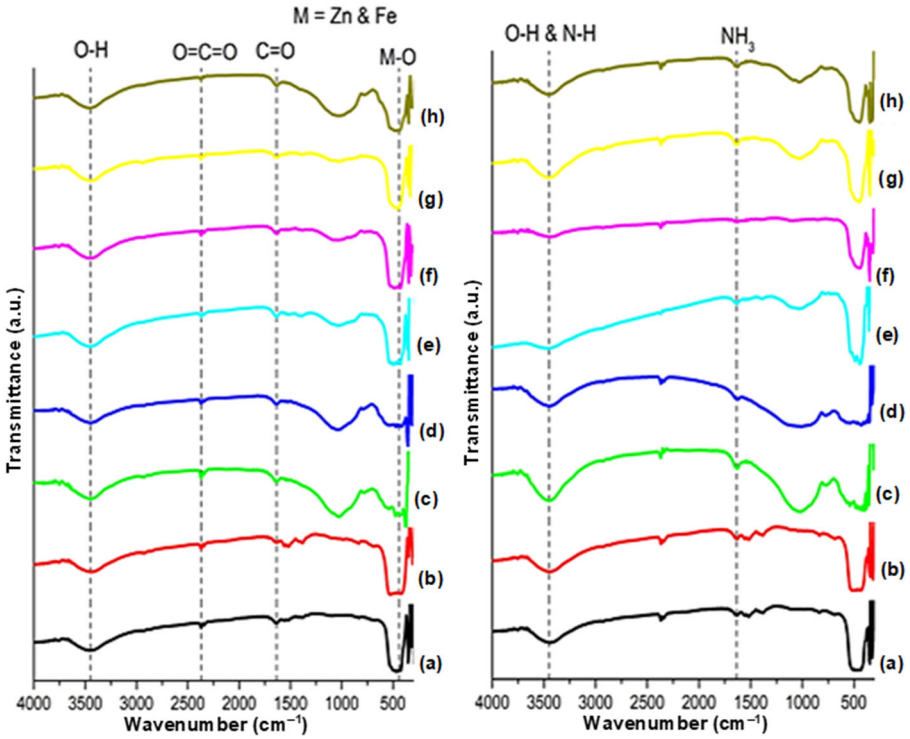

Fig 2. FTIR spectra (a) ZnO, (b) ZnO-MW, (c) BS, (d) BS-MW, (e) ZnO-BS-1-OV, (f) ZnO-BS-1-MW, (g) ZnO-BS-2-MW, and (h) ZnO-BS-4-MW before (left side) and after (right side) ammonia adsorption

1473.62–1635.64 cm^{-1} may be considered as the bending vibration of NH_3 molecules because it is identical to that found in the coordinately bonded NH_3 molecules. However, the intensity of this absorption band decreases in parallel with the decrease of the broadband at 3448.72–3456.44 cm^{-1}, which suggests that the bending vibration is of the weakly adsorbed NH_3 molecules. The appearance of the absorption band at 1473.62 cm^{-1} implies the formation of NH_4^+ ions on the surface of the catalyst. The situation resembles the case of the adsorption of NH_3 on the α-Fe_2O_3 surface, where NH_4^+ ions are formed by the interaction of NH_3 molecules with physisorbed H_2O on α-Fe_2O_3 [29]. This absorption appears in the same area as the C=O vibration so that it is possible to overlap each other.

The surface morphology of ZnO-BS-1-OV and ZnO-BS-1-MW is illustrated in Fig. 3. These morphological structures can be the evidence to show that ZnO and sand have been mixed and interacted well. The materials proved to be hexagonal-cubic which supported the previous XRD data.

The TEM image of ZnO-BS-1-OV is shown in Fig. 4. TEM studies were carried out to understand the shape characteristics of the crystals. The image confirms that the particles are mostly cubic with slightly hexagonal, which corroborates the previous XRD and SEM data.

From Fig. 5, both materials exhibit Type IV isotherms related to the characteristics of mesoporous materials, according to the IUPAC classification. This typical mesoporous material is represented by the presence of a hysteresis loop at the isotherm. The type of hysteresis possessed by these materials follows the H3 pattern described by IUPAC. The desorption branch tends to be perpendicular to the adsorption branch in the closure region at lower relative pressures. In the hysteresis loop H3, the pores have a wedge or slit geometry, resulting from agglomerates of parallel plates-shaped particles [30].

The surface area was calculated using the BET approach, while the pore diameter and volume were calculated using the BJH. Based on the calculation results in Table 4, the surface area of ZnO-BS-1-MW is

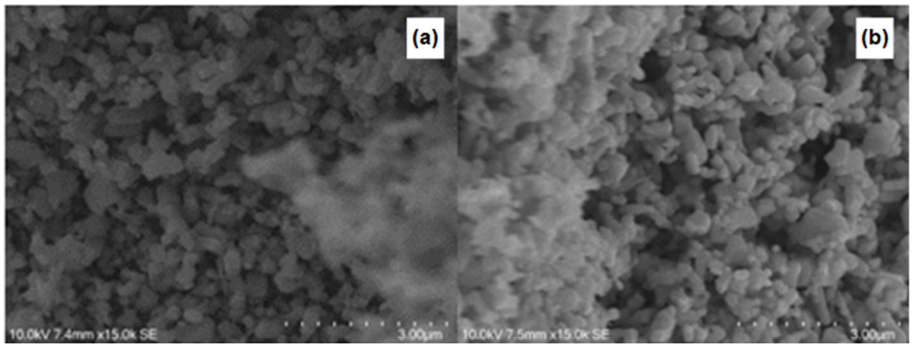

Fig 3. SEM micrographs of (a) ZnO-BS-1-OV and (b) ZnO-BS-1-MW

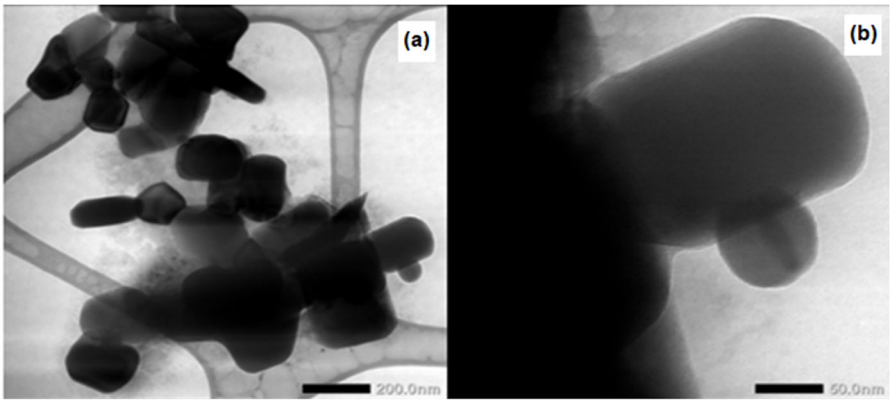

Fig 4. TEM image of ZnO-BS-1-OV in (a) 20,000 and (b) 80,000 times magnification

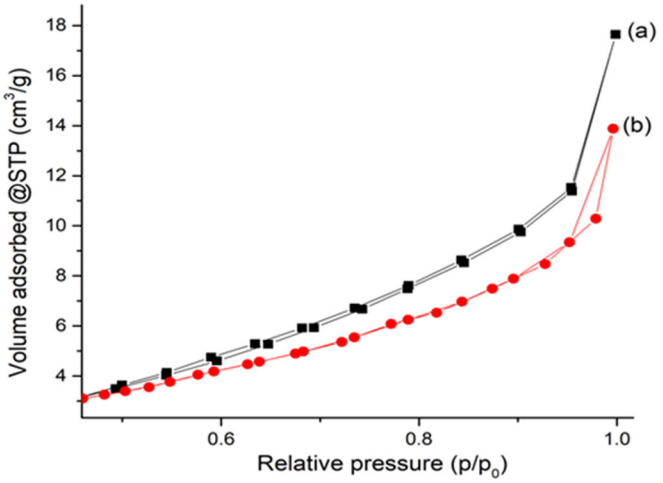

Fig 5. N_2 adsorption-desorption isotherm of (a) ZnO-BS-1-OV and (b) ZnO-BS-1-MW

larger than that of ZnO-BS-1-OV. This value follows the crystallite size of XRD, where a small crystal size will produce a large surface area. This indicates that heating by microwave also affects the textural properties of the material. The resulting pore diameter is also in the mesoporous range, which is between 2–50 nm. This value confirms the appearance of a hysteresis loop on the nitrogen isotherm curve.

The observation of magnetic properties was conducted by attracting each material using an external magnetic field. The more easily attracted indicates that the material is more easily separated from the reaction. Based on Fig. 6, materials containing more BS will be attracted more easily than pure ZnO. This is because the magnetic properties arise from the iron oxides naturally present in the BS material. These magnetic properties also offer benefits for catalyst separation and reuse for ODS to meet the principles of green chemistry. However, the ZnO-BS material was not completely attracted by the magnet. This is based on the method used, namely physical mixing, not chemical reactions so that the resulting interaction between ZnO and BS is only a physical bond.

Catalytic Activity Test

The reaction time chosen for the oxidative desulfurization of dibenzothiophene (ODS-DBT) was 20 min after the addition of H_2O_2. From the literature, insignificant sulfur removal was witnessed after 60 min of reaction time, exceeding to longest tested time (240 min). It was anticipated that at prolonged reaction

Table 4. Textural properties of ZnO-BS-1-OV and ZnO-BS-1-MW

Material	Surface area (m^2/g)	Pore volume (cm^3/g)	Pore diameter (nm)
ZnO-BS-1-OV	6.649	0.025	15.259
ZnO-BS-1-MW	7.268	0.019	10.715

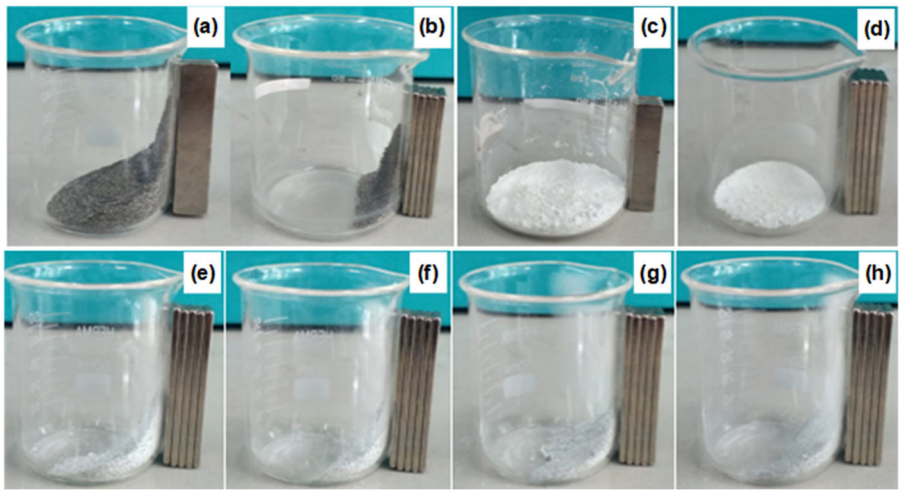

Fig 6. Magneticity test of (a) BS, (b) BS-MW, (c) ZnO, (d) ZnO-MW, (e) ZnO-BS-1-OV, (f) ZnO-BS-1-MW, (g) ZnO-BS-2-MW, and (h) ZnO-BS-4-MW

time, the reaction does not affect the proportion of desulfurization due to the degradation of most oxidants. Quantitative analysis through titration method discovered that most of H_2O_2 were utilized after reaction, either through selective utilization or unselective utilization due to (i) decomposition to oxygen and water, (ii) hydrogenation to water, and (iii) direct non-selective formation of water.

The operation temperature chosen was 60 °C because the model fuel (n-hexane) is evaporated at higher temperatures. Besides, high temperatures will initiate the non-selective decomposition of H_2O to produce O_2 and H_2O, subsequently suppressing the oxidation capability [31]. Availability of the H_2O_2 throughout the reaction is crucial since it will form an active species that is capable of oxidizing sulfur to sulfoxide and sulfone. Another reason was the sulfur removal appeared to be unsatisfying at a temperature of 40 °C from Li and Liu's research, which may be because H_2O_2 and the catalyst cannot work efficiently under low reaction temperature [32]. Raising the reaction temperature from 40 to 60 °C led to a remarkable increase in sulfur removal. However, a further increase of the reaction temperature to 70 °C caused a decrease in the desulfurization efficiency. This is because the high temperature leads to the partial decomposition of H_2O_2, which brings down the oxidation efficiency.

The concentrations of DBT were analyzed using a UV spectrophotometer. The phase fractional was taken from the n-hexane phase for DBT analysis. After the reaction, the oxidized DBT was separated by decantation after collecting the catalyst by an external magnetic field. Then, the DBT concentration in the hydrocarbon layer was calculated by UV-Vis spectrophotometer. The absorption at 279 nm was used to monitor the DBT concentration based on the scanning of DBT solution to find the maximum wavelength of DBT in *n*-hexane solution. The highest absorbance found was 3.629 in wavelength of 279 nm. Therefore, 279 nm was chosen as a maximum wavelength to further observe the absorbance found in oxidized DBT.

The catalytic ODS-DBT process consists of two steps. In the first step, sulfur-containing fuel oil (in this case, DBT in n-hexane solution) was subjected to catalytic oxidation to produce oxidized sulfur compounds (sulfones/sulfoxides) in the presence of an oxidant (H_2O_2). In the second step, the oxidized sulfur compounds were removed from the reaction mixture using the liquid/liquid extraction method. In this research, a highly polar solvent, acetonitrile, was used to extract the sulfur compounds [33].

Table 5 shows that Microwave treatment on the material can reduce the catalytic activity as happened in ZnO-BS-1-OV→ZnO-BS-1-MW, BS→BS-MW, and ZnO→ZnO-MW. In addition, the higher BS or lower ZnO content in the mixture was able to increase the catalytic activity. It might happen due to the availability of Fe=O catalytic sites present in BS responsible for activating iron superoxide for the oxidation reaction. Other contents in BS, such as silica and alumina oxide, may also work synergistically with iron oxide. The highest DBT removal efficiency is shown by the use of ZnO-BS-1-OV as a catalyst due to its highest acidity.

The ZnO-BS-1-OV catalyst has shown to be efficient in the removal of DBT compounds. It is believed that the reaction was initiated by nucleophilic attack of H_2O_2 by the Fe=O bond of ZnO-BS-1-OV catalyst surface, which had generated active intermediate iron peroxides. Then, nucleophilic attack of the sulfur atom with higher electron density in DBT on iron peroxide was conducted to form sulfoxide and regenerated Fe=O where the sulfoxide later undergoes further oxidation by using iron peroxide that converts it to a corresponding sulfone and regenerates Fe=O for a close cycle of reaction. This mechanism demonstrates that the presence of active Fe=O sites is important for an

Table 5. Catalytic activity in ODS and Non-ODS of DBT

Material	Removal of DBT (%)	
	ODS	Non-ODS
ZnO	74.17	-
ZnO-MW	73.61	-
BS	79.24	-
BS -MW	74.36	-
ZnO-BS-1-OV	81.59	75.27
ZnO-BS-1-MW	70.54	-
ZnO-BS-2-MW	71.53	-
ZnO-BS-4-MW	71.53	-

efficient ODS reaction. Thus, ZnO-BS-1-OV with a higher amount of Fe justifies the availability of more Fe=O sites compared to other ZnO-BS catalysts.

The efficiency of ODS-DBT was also known as the activity of the catalyst. It was shown that the efficiency of ODS-DBT increase with the increase of the acidity of the catalyst. Interaction between H_2O_2 and acidic sites of the catalyst improves the electrophilic attack of H_2O_2 on DBT as a weak nucleophile, forming intermediary per-oxometallic complex on the catalyst surface, thus increasing the efficiency of ODS-DBT. The ZnO-BS-1-OV showed the highest catalytic activity because of its highest acidity, while the ZnO-BS-1-MW showed the lowest catalytic activity due to the lowest acidity.

Furthermore, the ZnO-BS-1-OV catalyst will be reused to compare its activity in ODS and non-ODS reactions. From the research results in Table 5, the addition of H_2O_2 as an oxidizing agent can increase the efficiency of DBT removal. This is supported by the presence of iron oxide contained in BS capable of activating oxidants. It is important to highlight that during the oxidation process, few bubbles were observed when the fresh catalyst was immersed in the DBT solution, indicating the presence of O_2 gas originated from the decomposition of hydrogen peroxide.

The ability to remove the sulfur compound without altering the hydrocarbon structure is crucial in preserving the quality of fuel. Detail analysis on FTIR had been discovered, and it confirmed that all the catalysts are not affecting the main structure of the treated fuel.

Fig. 7 shows the FTIR spectra comparison between the DBT and oxidized DBT. Both compounds show almost identical bands, except that the two new bands at nearly 964.61 cm^{-1} at the ZnO-BS-1-OV that can be assigned as the asymmetrical and symmetrical stretching vibration modes of sulfoxide [34] and band at 1064.71 and 1056.99 cm^{-1} in all samples correspond to the S=O bond of sulfone [35]. Thus, it confirmed that the oxidation process successfully occurred and produced an oxygenated sulfur compound. Some of these functional groups are still shown in the upper layer after the extraction process due to the removal of DBT is not 100% based on the results in UV-visible spectrometry. Other

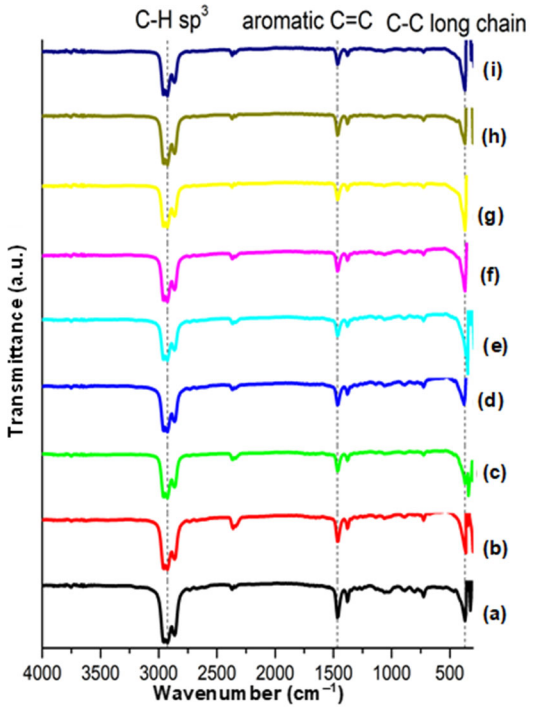

Fig 7. DBT solution (a) before ODS and after ODS using (b) ZnO (c) ZnO-MW (d) BS (e) BS-MW (f) ZnO-BS-1-OV (g) ZnO-BS-1-MW (h) ZnO-BS-2-MW (i) ZnO-BS-4-MW

bands shown in the FTIR spectra are 2954.95–2862.36 cm^{-1} correspond to the C–H sp^3, 1465.90–1381.03 cm^{-1} correspond to the aromatic C=C, and 370.33–324.04 cm^{-1} correspond to the C–C long-chain [36].

■ CONCLUSION

Microwave treatment on the material can reduce acidity and crystallinity level but increase the crystallite size. High BS content or low ZnO content in ZnO-BS-MW material can increase acidity and reduce crystallinity level as well as crystallite size. Although the surface area of ZnO-BS-1-OV is smaller than that of ZnO-BS-1-MW, the material can produce the highest catalytic activity in ODS-DBT. This proves that the acidity of the catalyst dramatically affects the efficiency of DBT removal. The presence of iron oxide in the beach sand (BS) material, in addition to functioning to activate oxidant H_2O_2, also offers benefits for the separation of catalysts after the ODS reaction.

■ ACKNOWLEDGMENTS

The authors would like to thank all the members involved in the *Program Penelitian Kolaborasi Indonesia* (PPKI) 2021 project collaboration between Sebelas Maret University, Sepuluh Nopember Institute of Technology, and Universitas Gadjah Mada. This research project is fully funded by Universitas Gadjah Mada under the scheme of *Program Penelitian Kolaborasi Indonesia* (PPKI) 2021 with the contact number: 1070/UN1/DITLIT/DIT-LIT/PT/2021 for Wega Trisunaryanti.

■ REFERENCES

[1] Mohan, D., Pittman, C.U., and Steele, P.H., 2006, Pyrolysis of wood/biomass for bio-oil: A critical review, *Energy Fuels*, 20 (3), 848–889.

[2] Betiha, M.A., Rabie, A.M., Ahmed, H.S., Abdelrahman, A.A., and El-Shahat, M.F., 2018, Oxidative desulfurization using graphene and its composites for fuel containing thiophene and its derivatives: An update review, *Egypt. J. Pet.*, 27 (4), 715–730.

[3] Alizadeh, A., Fakhari, M., Khodeai, M.M., Abdi, G., and Amirian, J., 2017, Oxidative desulfurization of model oil in an organic biphasic system catalysed by Fe_3O_4@SiO_2-ionic liquid, *RSC Adv.*, 7 (56), 34972–34983.

[4] Dutta, A.M., Saikia, B.K., and Baruah, B.P., 2012, Oxidative desulphurization of North-East Indian coals by using different metal ions/oxides as catalyst, *Int. J. Innovative Res. Dev.*, 1 (7), 214–220.

[5] Tang, L., Luo, G., Zhu, M., Kang, L., and Dai, B., 2013, Preparation, characterization and catalytic performance of HPW-TUD-1 catalyst on oxidative desulfurization, *J. Ind. Eng. Chem.*, 19 (2), 620–626.

[6] Yun, G.N. and Lee, Y.K., 2013, Beneficial effects of polycyclic aromatics on oxidative desulfurization of light cycle oil over phosphotungstic acid (PTA) catalyst, *Fuel Process. Technol.*, 114, 1–5.

[7] Shen, C., Wang, Y.J., Xu, J.H., and Luo, G.S., 2015, Synthesis of TS-1 on porous glass beads for catalytic oxidative desulfurization, *Chem. Eng. J.*, 259, 552–561.

[8] Xiao, J., Wu, L., Wu, Y., Liu, B., Dai, L., Li, Z., Xia, Q., and Xi, H., 2014, Effect of gasoline composition on oxidative desulfurization using a phosphotungstic acid/activated carbon catalyst with hydrogen peroxide, *Appl. Energy,* 113, 78–85.

[9] Chen, Y., Zhao, S., and Song, Y.F., 2013, An efficient heterogeneous catalyst based on highly dispersed $Na_7H_2LaW_{10}O_{36}{\cdot}32H_2O$ nanoparticles on mesoporous silica for deep desulfurization, *Appl. Catal., A*, 466, 307–314.

[10] Wan Abu Bakar, W.A., Ali, R., Abdul Kadir, A.A., and Wan Mokhtar, W.N.A., 2012, Effect of transition metal oxides catalysts on oxidative desulfurization of model diesel, *Fuel Process. Technol.*, 101, 78–84.

[11] Guo, J.X., Fan, L., Peng, J.F., Chen, J., Yin, H.Q., and Jiang, W.J., 2014, Desulfurization activity of metal oxides blended into walnut shell based activated carbons, *J. Chem. Technol. Biotechnol.*, 89 (10), 1565–1575.

[12] Hassanpour, A., Hosseinzadeh-Khanmiri, R., Babazadeh, M., and Edjlali, L., 2016, ZnO NPs: An efficient and reusable nanocatalyst for the synthesis of nitrones from DAG using H_2O as a solvent at room-temperature, *Res. Chem. Intermed.*, 42 (3), 2221–2231.

[13] Dar, B.A., Mohsin, M., Basit, A., and Farooqui, M., 2013, Sand: A natural and potential catalyst in renowned Friedel Craft's acylation of aromatic compounds, *J. Saudi Chem. Soc.*, 17 (2), 177–180.

[14] Arellano, U., Wang, J.A., Timko, M.T., Chen, L.F., Paredes-Carrera, S.P., Asomoza, M., González-Vargas, O.A., and Llanos, M.E., 2014, Oxidative removal of dibenzothiophene in a biphasic system using sol-gel Fe–TiO_2 catalysts and H_2O_2 promoted with acetic acid, *Fuel*, 126, 16–25.

[15] Adeyi, A.A. and Aberuaga, F., 2012, Comparative analysis of adsorptive desulphurization of crude oil by manganese dioxide and zinc oxide, *Res. J. Chem. Sci.*, 2 (8), 14–20.

[16] Tang, Q., Lin, S., Cheng, Y., Liu, S., and Xiong, J.R., 2013, Ultrasound-assisted oxidative desulfurization

of bunker-C oil using *tert*-butyl hydroperoxide, *Ultrason. Sonochem.*, 20 (5), 1168–1175.

[17] Omran, M., Fabritius, T., Heikkinen, E.P., and Chen, G., 2017, Dielectric properties and carbothermic reduction of zinc oxide and zinc ferrite by microwave heating, *R. Soc. Open Sci.*, 4 (9), 170710.

[18] Teh, P.F., Pramana, S.S., Kim, C., Chen, C.M., Chuang, C.H., Sharma, Y., Cabana, J., and Madhavi, S., 2013, Electrochemical reactivity with lithium of spinel-type ZnFe 2-$_y$Cr$_y$O$_4$ ($0 \leq y \leq 2$), *J. Phys. Chem. C*, 117 (46), 24213–24223.

[19] Zhu, W., Wu, P., Yang, L., Chang, Y., Chao, Y., Li, H., Jiang, Y., Jiang, W., and Xun, S., 2013, Pyridinium-based temperature-responsive magnetic ionic liquid for oxidative desulfurization of fuels, *Chem. Eng. J.*, 229, 250–256.

[20] Piscopo, C.G., Tochtermann, J., Schwarzer, M., Boskovic, D., Maggi, R., Maestri, G., and Loebbecke, S., 2018, Titania supported on silica as an efficient catalyst for deep oxidative desulfurization of a model fuel with exceptionally diluted H_2O_2, *React. Chem. Eng.*, 3 (1), 13–16.

[21] Ercuta, A., and Chirita, M., 2013, Highly crystalline porous magnetite and vacancy-ordered maghemite microcrystals of rhombohedral habit, *J. Cryst. Growth*, 380, 182–186.

[22] Cambier, P., 1986, Infrared study of goethites of varying crystallinity and particle size: II. Crystallographic and morphological changes in series of synthetic goethites, *Clay Miner.,* 21 (2), 201–210.

[23] Namduri, H., and Nasrazadani, S., 2008, Quantitative analysis of iron oxides using Fourier transform infrared spectrophotometry, *Corros. Sci.*, 50 (9), 2493–2497.

[24] Long, T., Yin, S., Takabatake, K., Zhnag, P., and Sato, T., 2009, Synthesis and characterization of ZnO nanorods and nanodisks from zinc chloride aqueous solution, *Nanoscale Res. Lett.*, 4 (3), 247–253.

[25] Khanna, L., and Verma, N.K., 2013, Size-dependent magnetic properties of calcium ferrite nanoparticles, *J. Magn. Magn. Mater.*, 336, 1–7.

[26] Parvin, T., Keerthiraj, N., Ibrahim, I.A., Phanichphant, S., and Byrappa, K., 2012, Photocatalytic degradation of municipal wastewater and brilliant blue dye using hydrothermally synthesized surface-modified silver-doped ZnO designer particles, *Int. J. Photoenergy*, 2012, 670610.

[27] Pholnak, C., Sirisathitkul, C., Suwanboon, S., and Harding, D.J., 2014, Effects of precursor concentration and reaction time on sonochemically synthesized ZnO nanoparticles, *Mater. Res.*, 17 (2), 405–411.

[28] Franco, R.L.M., Oliveira, T.G., Pedrosa, A.M.G., Naviciene, S., and Souza, M.J.B., 2013, Textural properties of nickel, palladium and titanium oxides supported on MCM.41 materials and their application on oxidative desulfurization of dibenzothiophene, *Mater. Res.*, 16 (6), 1449–1456.

[29] Adam, F., Jeannot, F., Dupre, B., and Glettzer, C., 1988, The remarkable effect of water vapour on the cracking of hematite during its reduction into magnetite, *React. Solids*, 5 (2-3), 115–127.

[30] Thommes, M., Kaneko, K., Neimark, A.V., Olivier, J.P., Rodriguez-Reinoso, F., Rouquerol, J., and Sing, K.S.W., 2015, Physisorption of gases, with special reference to the evaluation of surface area and pore size distribution (IUPAC Technical Report), *Pure Appl. Chem.*, 87 (9-10), 1051–1069.

[31] Zhang, X., Zhu, Y., Huang, P., and Zhu, M., 2016, Phosphotungstic acid on zirconia-modified silica as catalyst for oxidative desulfurization, *RSC Adv.*, 6 (73), 69357–69364.

[32] Li, B., and Liu, Z., 2011, "Synthesis and Characterization of Ordered Mesoporous Silica Pillared Clay with HPW Heteropoly Acid Encapsulated into the Framework and Its Catalytic Performance for Deep Oxidative Desulfurization of Fuels" in *Metal, Ceramic and Polymeric Composites for Various Uses*, Eds. Cuppoletti, J., InTechOpen, Rijeka, 225–238.

[33] Hossain, M.N., Choi, M.K., Park, H.C., and Choi, H.S., 2020, Purifying of waste tire pyrolysis oil using an S-ZrO_2/SBA-15-H_2O_2 catalytic oxidation method, *Catalysts*, 10 (4), 368.

[34] Calligaris, M., 2004, Structure and bonding in metal sulfoxide complexes: An update, *Coord. Chem. Rev.*, 248 (3-4), 351–375.

[35] Shakirullah, M., Ahmad, I., Ishaq, M., and Ahmad, W., 2009, Study on the role of metal oxides in desulphurization of some petroleum fractions, *J. Chin. Chem. Soc.*, 56 (1), 107–114.

[36] Abdul-Kadhim, W., Deraman, M.A., Abdullah, S.B., Tajuddin, S.N., Yusoff, M.M., Taufiq-Yap, Y.H., and Rahim, M.H.A., 2017, Efficient and reusable iron-zinc oxide catalyst for oxidative desulfurization of model fuel, *J. Environ. Chem. Eng.*, 5 (2), 1645–1656.